Journal of Hydrology 519 (2014) 1859–1869

Contents lists available at ScienceDirect

Journal of Hydrology

journal homepage: www.elsevier.com/locate/jhydrol

# An integrated modeling system for estimating glacier and snow melt driven streamflow from remote sensing and earth system data products in the Himalayas

M.E. Brown [a,*], A.E. Racoviteanu [b], D.G. Tarboton [c], A. Sen Gupta [c], J. Nigro [a,d], F. Policelli [a], S. Habib [a], M. Tokay [d], M.S. Shrestha [e], S. Bajracharya [e], P. Hummel [f], M. Gray [f], P. Duda [f], B. Zaitchik [g], V. Mahat [h], G. Artan [i], S. Tokar [j]

[a] NASA Goddard Space Flight Center, Greenbelt, MD, USA
[b] Laboratoire de Glaciologie et Géophysique de l'Environnement, France
[c] Utah State University, Logan, UT, USA
[d] Science Systems and Applications, Inc., Lanham, MD, USA
[e] International Centre for Integrated Mountain Development (ICIMOD), Kathmandu, Nepal
[f] AquaTerra Consultants, Decatur, GA, USA
[g] Johns Hopkins University, Baltimore, MD, USA
[h] Colorado State University, USA
[i] U.S. Geological Survey, Sioux Falls, SD, USA
[j] U.S. Agency for International Development, Office of Foreign Disaster Assistance, Washington, DC, USA

ARTICLE INFO

*Article history:*
Received 6 May 2014
Received in revised form 14 September 2014
Accepted 18 September 2014
Available online 30 September 2014
This manuscript was handled by Geoff Syme, Editor-in-Chief

*Keywords:*
Himalayas
Glacier melt
Energy balance
Stream flow

SUMMARY

Quantification of the contribution of the hydrologic components (snow, ice and rain) to river discharge in the Hindu Kush Himalayan (HKH) region is important for decision-making in water sensitive sectors, and for water resources management and flood risk reduction. In this area, access to and monitoring of the glaciers and their melt outflow is challenging due to difficult access, thus modeling based on remote sensing offers the potential for providing information to improve water resources management and decision making. This paper describes an integrated modeling system developed using downscaled NASA satellite based and earth system data products coupled with in-situ hydrologic data to assess the contribution of snow and glaciers to the flows of the rivers in the HKH region. Snow and glacier melt was estimated using the Utah Energy Balance (UEB) model, further enhanced to accommodate glacier ice melt over clean and debris-covered tongues, then meltwater was input into the USGS Geospatial Stream Flow Model (GeoSFM). The two model components were integrated into Better Assessment Science Integrating point and Nonpoint Sources modeling framework (BASINS) as a user-friendly open source system and was made available to countries in high Asia. Here we present a case study from the Langtang Khola watershed in the monsoon-influenced Nepal Himalaya, used to validate our energy balance approach and to test the applicability of our modeling system. The snow and glacier melt model predicts that for the eight years used for model evaluation (October 2003–September 2010), the total surface water input over the basin was 9.43 m, originating as 62% from glacier melt, 30% from snowmelt and 8% from rainfall. Measured streamflow for those years were 5.02 m, reflecting a runoff coefficient of 0.53. GeoSFM simulated streamflow was 5.31 m indicating reasonable correspondence between measured and model confirming the capability of the integrated system to provide a quantification of water availability.

Published by Elsevier B.V.

## 1. Introduction

The Hindu Kush Himalayan (HKH) region possesses a large resource of snow and ice, which act as a freshwater reservoir for irrigation, domestic water consumption or hydro-electric power for billions of people in Asia. Snow and glacier-melt represent a significant source of surface water and influence many aspects of hydrology including water supply, erosion and flood control (National Research Council, 2012). With projected climate-induced changes in snow and ice and population growth, the region is at risk of experiencing water stress in the coming years (Immerzeel

* Corresponding author.
*E-mail address:* molly.brown@nasa.gov (M.E. Brown).

http://dx.doi.org/10.1016/j.jhydrol.2014.09.050
0022-1694/Published by Elsevier B.V.

et al., 2010, 2012; Kaser et al., 2010). There are, in particular, concerns about the effect of climate change on snow water equivalent, snowmelt runoff, glacier melt runoff and total streamflow and their distribution due to mean global temperature increases.

Some recent studies published the impact of temperature increase on glacier melt runoff high altitude basins (Barnett et al., 2005; Singh and Kumar, 1997a,b), but these tend to be over-estimated or conducted on small basins (Savoskul and Smakhtin, 2013). Research has shown that there are significant differences across the HKH region with regard to the contribution of glacier and snow melt to hydrological systems, changes in the timing or amount of snowmelt due to increasing temperatures or decreasing winter precipitation due to climate change. These changes may have far-reaching societal consequences, particularly in Asia (Bookhagen and Burbank, 2010; Immerzeel et al., 2012). More information is needed to monitor and anticipate snow and glacier ice melt runoff at larger scales to improve water resources management and flood protection (Jeuland et al., 2013).

The monitoring capability of hydrologic resources in this region is challenged by the difficulty of installing and maintaining a climate and hydrologic monitoring network, due to limited transportation and communication infrastructure and difficult access to glaciers. As a result of the high, rugged topographic relief, ground observations in the region are extremely sparse (Lo et al., 2011). For example, only a few glaciers are currently monitored for mass balance measurements in the Himalaya (Dobhal et al., 2008; Wagnon et al., 2007, 2013). In the recent years, remote sensing-based modeling has helped provide has been increasingly used in recent years to estimate water resources (Thayyen and Gergan, 2010) and thus has helped improve water resources decision making and management in these data-scarce areas.

While some progress has been made in understanding the contribution of snow and ice melt to streamflow in the Himalaya using degree-day or simple ablation models (Immerzeel et al., 2010, 2012; Racoviteanu et al., 2013), a region-wide estimate of water resources is hampered by the fact that these models are not in public domain, coupled with lack of access or technical expertise of local institutions. Another significant barrier for decision makers in monitoring and understanding the impact of climate-induced changes in snow and glaciers on water resources is the scientific disciplinary divide that isolates glacier experts and hydrological analysts, as well as lack of integrated tools that allow institutional actors trusted by decision makers to conduct analyses themselves. Developing a tool that can address all these limitations by integrating snow, ice and precipitation information from both satellite and local sources is critical to allow appropriate response to natural hazards to the population (Wisner et al., 2004), and is a focus of this study.

Here we present an integrated modeling capability developed to meet the water resources planning needs of this broad, multi-nation region taking full advantage of NASA Earth Science data and modeling products. We developed a hydrologic tool that can be used at basin or sub-basin scale in an easy-to-use graphical user interface framework accessible to most users. The modeling needs were addressed by integrating an enhanced, gridded version of the Utah Energy Balance (UEB) snowmelt model, denoted here as UEB-Grid and the Geospatial Stream Flow Model (GeoSFM) into the Better Assessment Science Integrating point and Nonpoint Sources (BASINS) modeling system. We downscaled various NASA gridded remote sensing and climate products and combined them with higher-resolution data for use in these models.

The resulting tool, publicly available to both the hydrological and cryospheric communities online (http://hspf.com/pub/HIMALA_BASINS/) is referred here as HIMALA BASINS, and will be maintained in conjunction with the U.S. Environmental Protection Agency's (EPA) open-source BASINS tool. The HIMALA BASINS model grew out of a decade of collaborative work between USAID's Office of Foreign Disaster Assistance, USGS and ICIMOD and was initially funded through the Asia Flood Network, a project designed to produce satellite-derived rainfall data products used to drive hydrological models. Since 2003, the NOAA Climate Prediction Centre's RFE2 (Xie et al., 2002) products have been validated by ICIMOD (Shrestha, 2010) within the hydrological model GeoSFM (Artan et al., 2007). ICIMOD has been training collaborators from its member countries to use these products. Here, we address the need to augment the GeoSFM with a capability to model water melt from snow and glacier ice, which was previously not taken into account in earlier versions of this model.

The novelty of HIMALA BASINS tool consists in allowing the user to isolate various components of streamflow (rainfall, snow and glacier ice melt) in a cost-free, open-source graphical-user interface-based system that can be used for government and institutional decision-making. Given the limitations in the spatial frequency, temporal resolution and accuracy of satellite data, this study does not claim to provide the most accurate estimate of the streamflow components at large scales in the HKH region. Rather, we focus on developing and validating a tool that is capable of integrating glacier melt components as well as high-resolution climate data when available. In this paper we focus on the methodology used to integrate UEB and GeoSFM into a seamless product, illustrated for eight years of simulations. A more thorough description of the model results is presented elsewhere Sen Gupta (2014).

Our study addresses two needs: (1) to improve the understanding of the contribution of snow and ice to Himalayan water resource and (2) to assist with improved management of water resources, evaluation of projected of climate change impacts on water resources, and advanced modeling and data assimilation capability available to users in the Himalayan region. Here we present results from a very high altitude, highly glaciated region where we document the contribution of snow and ice melt to streamflow and demonstrate the importance using an integrated model for these regions. The paper is structured as follows: we first describe the integration of the two models (UEB and GeoSFM) into the BASINS modeling framework; we then describe the satellite data products, downscaling algorithms and glacier mapping methods, and finally we present model results and discussion for the Langtang Khola case study in the Nepal Himalaya.

## 2. Study site

The test site for the HIMALA BASINS methodology is the Langtang Khola Watershed in Nepal Himalaya, covering a surface of 360 $km^2$, with an elevation range of 3737 m to 7174 m (Fig. 1). Various research studies focused on the contribution of snow and ice-melt to streamflow in the Langtang Khola watershed (Immerzeel et al., 2010, 2012; Racoviteanu et al., 2013). We chose Langtang Khola as a validation site due to the availability of climate records from Nepal Department of Hydrology and Meteorology (DHM), as well as for comparison with these past studies, using different methodology. The prototype system was tested on this watershed by the HIMALA team while further evaluation of the system is being conducted by ICIMOD and the partners from regional member countries in larger basins in the HKH region (Narayani, Manas and Jhelum basins).

## 3. Modeling framework: HIMALA BASINS

In this study, we linked a snow melt model with a stream flow model within a version of the BASINS software developed and maintained at U.S. EPA. BASINS consists of a pre-existing suite of hydrological models and supporting tools, and was chosen for this

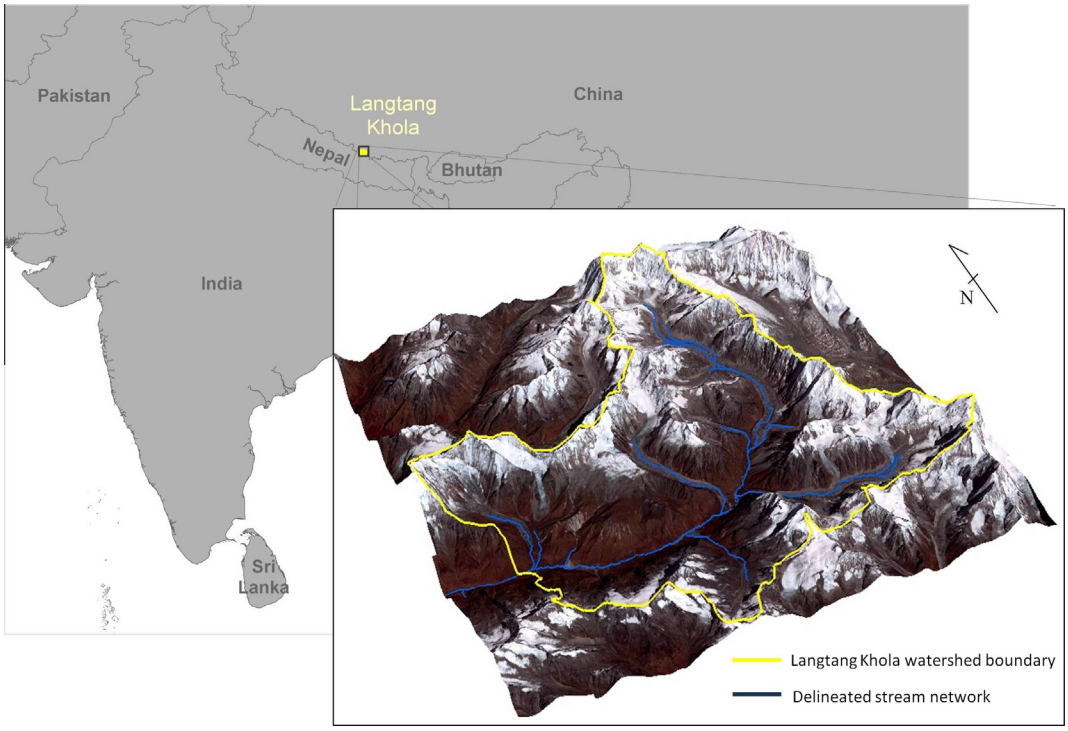


**Fig. 1.** Langtang Khola watershed in the Koshi in Nepal where HIMALA BASINS test data was developed and evaluated.

project due to its implementation using the MapWindow Geographic Information Systems (GIS). HIMALA BASINS incorporates two models: the UEBGrid (for estimating meltwater components) and GeoSFM models (for hydrologic modeling and routing), both of which were implemented as BASINS plugins by AQUA TERRA Consultants, the prime contractor for development and support of BASINS. The HIMALA BASINS version of BASINS is fully available to users via free download at http://hspf.com/pub/HIMALA_BASINS/. The HIMALA BASINS User's Manual (located in the documentation folder at the same URL) guides the user through each component so that one component builds on another beginning with the preprocessing and downscaling routines, building UEBGrid-required layers in GeoSFM, running the UEBGrid, and finally running the GeoSFM program. The acquisition of data is discussed when introducing each component within the manual so that the input data required for each model are not confused. Running the UEBGrid and GeoSFM independently is also described in the manual.

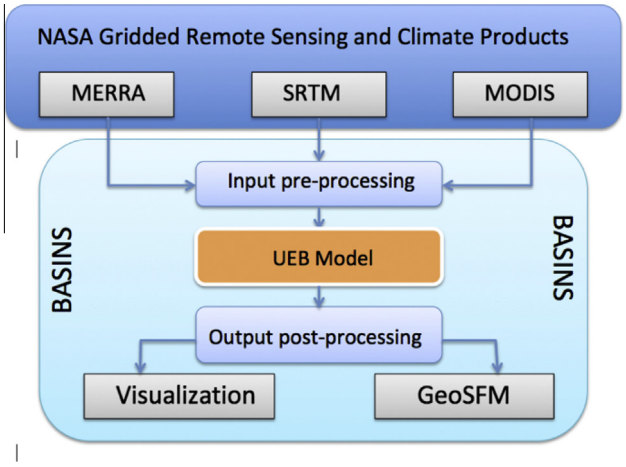


**Fig. 2.** General modeling framework of HIMALA BASINS system, integrating UEB with GeoSFM.

### 3.1. Data sources and downscaling algorithms

To estimate the effectiveness of using both the UEB and GeoSFM within the same framework, we combined NASA gridded climate data and remote sensing products with higher resolution elevation data for use with the model (Fig. 2). Below we describe these data sources as well as the preprocessing scripts that were developed to extract and downscale NASA products into the format required for these models.

#### 3.1.1. Climate data

Climate data used to drive the snow and ice melt model was derived from MERRA and RFE2 data sources (Table 1). We developed downscaling methods for temperature, precipitation, wind speed, relative humidity, shortwave and longwave radiation (Fig. 3) to match the 90-m scale of the melt model, chosen based on the Shuttle Radar Topography Mission (SRTM) elevation data described below. This high resolution is required to estimate glacier and snow melt appropriately in our high altitude glaciated basin. The downscaling methods were implemented in R (Bates et al., 2012).

Because of the lack of comprehensive meteorological data in the basin, we chose to use MERRA inputs. MERRA is a recent near-real time global climate reanalysis product developed at NASA, based on the Goddard Earth Observing System version 5 (GEOS-5), NASA general circulation model (Rienecker et al., 2011; Suarez et al., 2008) and National Centers for Environmental Prediction (NCEP) Gridpoint Statistical Interpolation (GSI) analysis (Wu et al., 2002). MERRA temperature, wind speed and relative humidity are reported at a height of 2 m above ground, at a spatial resolution of 2/3° longitude by 1/2° latitude, and hourly time resolution. Incoming shortwave and longwave radiation are reported at the

**Table 1**
Input data sources for BASINS UEB and GeoSFM models.

| Data | Type/resolution | Source | Frequency | Period |
|---|---|---|---|---|
| *Satellite data products* | | | | |
| MODIS land cover | MOD12Q1 500 m | NASA | Annual | 2000 to current |
| Precipitation (RFE-2) | Satellite/ground 0.1° × 0.1° | NOAA | Daily | 2001 to present |
| Leaf area index | MOD15, 1 km | NASA | Daily | 2000 to current |
| Percent Canopy Cover | MOD15, 500 m | NASA | Daily | 2000 to current |
| *Glaciers* | | | | |
| Glacier Outlines 2000 Debris versus Ice information | ASTER and Landsat 30 m | ICIMOD Calculated by team | Decadal | 2000 |
| *Hydrological parameters* | | | | |
| Digital Elevation Model | SRTM, 90 m | USGS | One time | 2000 |
| Soil Type | 1–5 million resolution | FAO | One time | 1960 |
| Evapotranspiration | Calculated from MERRA temperature data | NASA | Daily | 1979 to current |
| *Modeled data from GEOS-5 (MERRA)* | | | | |
| Air temperature | 0.5° × 0.66° resolution | NASA GMAO | Hourly | 1979 to current |
| Horizontal wind speed, | 0.5° × 0.66° | NASA GMAO | Hourly | 1979 to current |
| Relative humidity | 0.5° × 0.66° | NASA GMAO | Hourly | 1979 to current |
| Short-wave radiation | 1° × 1.25° | NASA GMAO | Hourly | 1979 to current |
| Long-wave radiation | 1° × 1.25° | NASA GMAO | Hourly | 1979 to current |
| *In situ* | | | | |
| Stream flow data at basin outlet | Langtang Khola observations | Nepal Meteorological Agency | Daily | 2001 to current |

surface, at coarser resolution of 1.0° by 1.25° and 3-hourly time step (Lucchesi, 2012). All MERRA records are available from 1979 to present.

MERRA hourly temperature data were averaged into three hour blocks, bilinearly interpolated and projected to 90-m using functions in the R raster library (Hijmans et al., 2013). They were also adjusted for elevation differences between the effective elevation determined from the geo-potential height that MERRA used and SRTM DEM elevation using a monthly lapse rate from Liston and Elder (2006). Relative humidity was calculated from MERRA specific humidity using a monthly dew point lapse rate, also from Liston and Elder (2006) and the same elevation differences as for temperature. Horizontal wind speed magnitude was obtained from eastward and northward wind components from MERRA and was interpolated and projected to 90-m resolution. MERRA reports three hourly incoming solar radiation at an elevation corresponding to the MERRA geo-potential height instead of the actual elevation from sea level. A pressure based atmospheric attenuation coefficient was calculated for each time step and used to adjust MERRA incoming solar-radiation to the grid SRTM DEM elevation using a standard atmosphere pressure elevation relationship. Incoming longwave radiation was calculated based on downscaled air temperature following the methods of Liston and Elder (2006).

We used daily total precipitation estimates from RFE2 data. These records were constructed using four observational input data sources, namely: approximately 280 GTS stations, geostationary infrared cloud top temperature fields, polar orbiting satellite precipitation estimate data from SSM/I, and AMSU-B microwave sensors (Xie et al., 2002). Near-real time daily rainfall estimations are available for the Southern Asian domain (70–110° East; 5–35° North) at a spatial resolution of 0.1° by 0.1° beginning on May 01, 2001. The RFE2 generally underestimates intense rainfall events and overestimates rainfall in rainshadow and arid areas (Shrestha, 2010). Comparing with gauge data, the RFE2 has daily rainfall bias of −1.1 mm/day over the period 2003–2006, with a root mean square error from gauges over the whole of Nepal of −4.0 mm/day (Shrestha, 2010). RFE2 daily precipitation data was divided into three-hourly precipitation increments assuming uniform precipitation within the day and bilinearly interpolated to the 90 m spatial resolution.

### 3.1.2. Elevation and glacier data

Elevation data came from the SRTM v.4 (CGIAR), a hydrologically-sound, void-filled DEM (CGIAR-CSI, 2004). The vertical accuracy of the SRTM DEM in this area, was reported as 31 m ± 10 m (Racoviteanu et al., 2013). An orthorectified ASTER scene from October 30, 2003 covering the entire Trishuli basin was used as a basis for delineating glacier outlines and variables needed as input in the melt model. The scene had high contrast over glaciers, minimal cloud cover, and was acquired at the end of the ablation season, so it was well-suited for computing a glacier albedo in absence of seasonal snow. Glacier outlines needed for the melt model were derived using semi-automatic methods (band ratios ¾ with a threshold of 2.0) described in detail elsewhere (Racoviteanu et al., 2008, 2009). Debris-covered ice was delineated manually using on-screen digitizing on false color composites (ASTER 321 and 543) and texture filters. Substrate albedo values for the glacier surface were determined from ASTER satellite reflectance values on a cell-by-cell basis using single-band to broad-band conversion algorithms (Greuell and Oerlemans, 2004; Greuell et al., 2002).

### 3.1.3. Land cover and soil data

Land cover data came from the MODIS Land Cover Type Yearly L3 Global 500-meter version 5.1 product (Fig. 3). The product is comprised of five classification schemes constructed from a year of MODIS Terra and Aqua observations using a supervised decision-tree classification method (Friedl et al., 2010). Land Cover Type 1, the International Geosphere-Biosphere Programme (IGBP) global vegetation classification scheme consisting of 17 classes, was used to derive appropriate land-cover based layers (canopy height, canopy structure, canopy cover fraction, leaf area index) needed to run UEBGrid and to compute basins response and flow distribution in GeoSFM. Since the rate of runoff generation and the rate of overland flow transport are influenced by land cover (Asante et al., 2007), these data are used in the model to compute vegetation roughness and overland velocity.

The GeoSFM requires soil data for basin characterization and model parameterization. Soil texture and depth, hydraulic conductivity, soil water holding capacity, maximum impervious area, and runoff curve number were estimated from the Digital Soil Map of the World produced by the U.N. Food and Agriculture Organization (FAO) and the U.N. Educational, Scientific and Cultural Organization

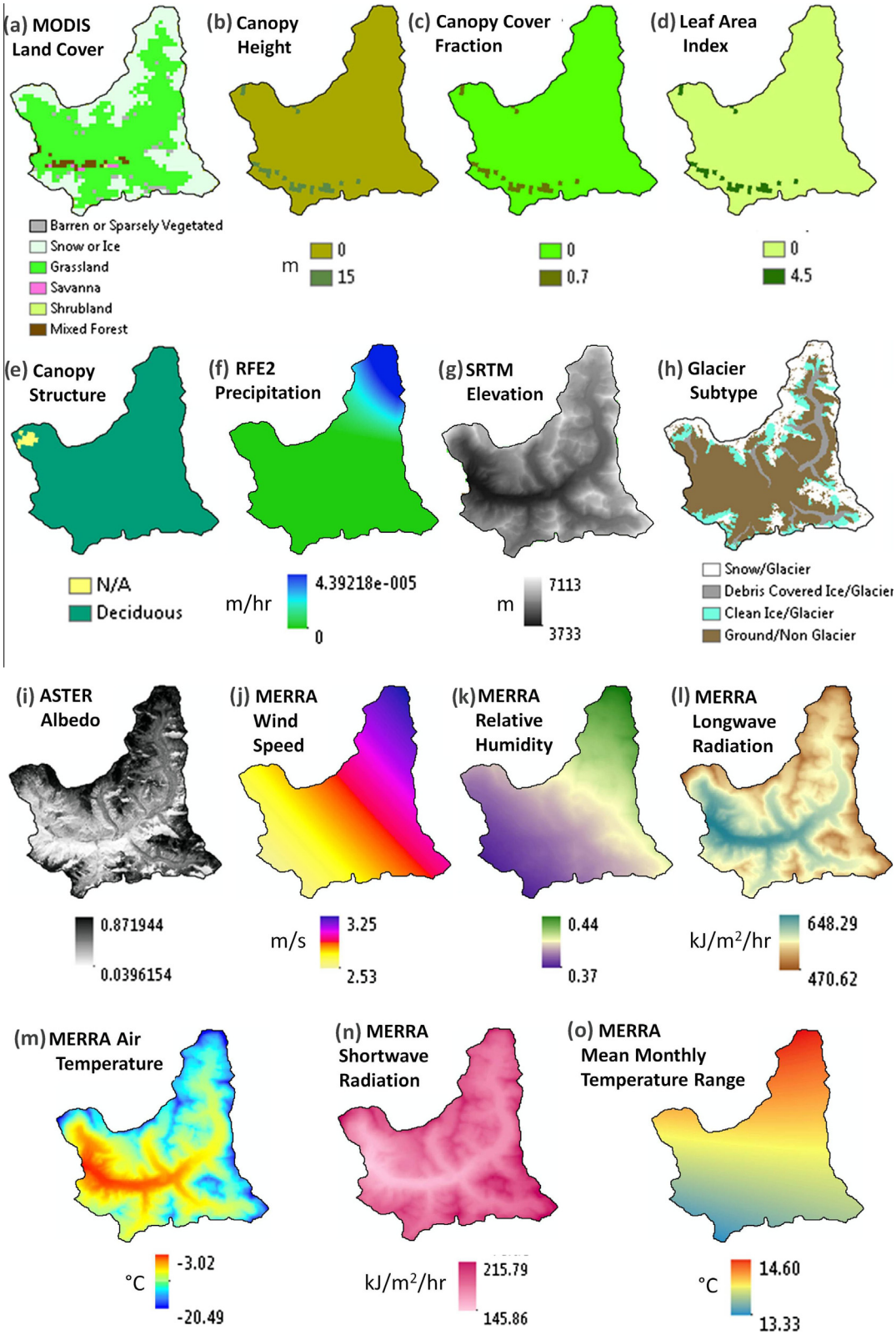


**Fig. 3.** Downscaled (90-m) UEBGrid model input: MERRA climatologic variables for a single 3-hour time step; RFE2 precipitation for a single 3-hour time step; ASTER-derived glacier subtype and albedo; CGIAR SRTM elevation data.

(UNESCO). Both land cover and soil data are used in GeoSFM to derive runoff curve numbers. These numbers are used to determine the amount of incident precipitation that becomes surface runoff (Asante et al., 2007).

The UEB requires canopy height, canopy coverage, leaf area index and canopy structure parameters in vegetated areas. A look up table is used to assign each of these for each grid cell based on the IGBP MODIS land cover classes, and parameter values are

written to netCDF files for each parameter. The majority of the Langtang Khola watershed is barren or glacier. Altitudes are too high for significant vegetation except in some of the lowest valleys where for 1.6% of the watershed MODIS landcover was classified as mixed forest (Fig. 3).

### 3.2. UEBGrid melt model

Snow and glacier ice melt was computed in this study using an enhanced version of the Utah Energy Balance (UEB) snowmelt model to which the capability to compute glacier melt has been added. UEB is a parsimonious, physically-based model that can be driven by readily available inputs and applied with no (or minimal) calibration. UEB was initially developed for the prediction of snowmelt rates that produce stream and river flows during the spring and summer (Tarboton et al., 1995; Tarboton, 1994) and evaluated at locations in California, Idaho, Utah and Colorado (Luce, 2000; Luce and Tarboton, 2004, 2010; Luce et al., 1998; Tarboton et al., 2000; You, 2004). In its initial form, the UEB model used a lumped representation of the snowpack with two primary state variables: snow water equivalent and energy content relative to a reference state of water in the ice phase at or below freezing. This energy content was used to determine snowpack average temperature or liquid fraction. Snow surface age was retained as a third state variable, and used for the calculation of surface albedo (Tarboton and Luce, 1996).

A vegetation component was developed for UEB to enable the evaluation of snowmelt in forested areas (Mahat and Tarboton, 2012, 2013; Mahat et al., 2013). The vegetation components were tested at the TW Daniel Experimental Forest (TWDEF), located about 30 miles North–East of Logan, Utah. With the addition of the vegetation component, a state variable quantifying intercepted snow water equivalent was added. The vegetation component describes physical processes of snow–vegetation–atmosphere interactions including parameterizations for the representation of transmission and attenuation of radiation through a forest canopy, precipitation interception and unloading, snowmelt and sublimation of intercepted snow, and turbulent energy exchanges between the ground surface, canopy, and atmosphere in the initial model. The addition of this component in the model has enhanced the models' physically based capability for modeling snow accumulation, melt, interception, sublimation, and unloading in a forested environment. UEB has been used in various hydrological studies including estimating snowmelt and sublimation in the high Atlas mountains in Morocco (Schulz and De Jong, 2004), analyzing potential climate change impacts in Sacramento/San Joaquin watershed (Knowles and Cayan, 2002) in the Western US, and assessing the surface meteorological variables most critical for snowmelt (Raleigh et al., 2008).

Glacier melt is driven by the balance of energy at the interface between glacier and atmosphere, which is controlled by meteorological conditions (temperature and radiation) above the glacier and the physical properties of the glacier itself. On one side, the atmosphere supplies energy for melt, and on the other side, the glacier surface influences air temperature due to snow/glacier properties and their variability, mainly the albedo effect (Hock, 2005). The relationship between the melt rate and short- and long-term mean temperature provides the basis for degree-day models, widely used to determine glacier melt in data-scarce areas of the world (Hock, 2003; Immerzeel et al., 2009, 2012; Kayastha et al., 1999, 2000; Singh et al., 2000a; Takeuchi et al., 2000). While simple degree-day models are useful for estimating melt based on temperature only, they have a limitation in that they do not take into account topographic effects (slope, aspect, and shading) that influence melt rates on a glacier. Energy balance models overcome these limitations. UEB was chosen for this study because it is a relatively simple energy balance model that parameterizes the snowpack using lumped (depth averaged) state variables so as to avoid having to model the complex processes that occur within a snowpack, while using a modified force-restore parameterization to capture physical differences between bulk (depth averaged) properties and the surface properties, which are important for calculating surface energy exchanges (see Table 2).

We extended the representations of surface energy balance fluxes in UEB to include the capability to quantify glacier melt on the basis of substrate type. Substrate is represented as one of: 0 – Ground/non-glacier, 1 – Clean glacier ice, 2 – Debris covered glacier ice and 3 – Glacier accumulation zone (snow). The amount of snow/ice melt is determined as follows: In the case of bare ground/non-glacier substrate type, the model tracks seasonal snow accumulation and ablation. In the glacier accumulation zone (snow surface) above the equilibrium line altitude, no melt is generated, as all precipitation is presumed to add to glacier accumulation. In the glacier ablation zone (comprised of clean or debris-covered ice), snow may accumulate on the glacier surface and then melt during the melting season. The model tracks seasonal snow accumulation and ablation in this area of the glacier in form of snow water equivalent. At each time step, the model computes the snowmelt, which is referred to as surface water input from snow melt (SWISM) until the seasonal snow on the ablation zone completely disappears. When seasonal snow water equivalent reaches zero, the surface energy balance is used to calculate the amount of glacier ice melt, which then becomes a component of the surface water input. The melted glacier ice is referred to as surface water input from glacier melt (SWIGM). Glacier ice melt is generated at the ice substrate only once seasonal snow covering glacier ice has melted. In addition, rain may occur both on bare ground as well as the glacierized parts of the watersheds. Surface water generated from rainfall is referred to as surface water input from rain (SWIR). The difference in functionality between debris covered and clean glacier ice surface is due only to the substrate albedo which is provided as an input.

This parameterization of glacier melt provides a simple, yet practical way to quantify energy balance driven glacier melt given the information available. It neglects a number of physical processes for which there is limited information. Debris cover on glaciers, influences the melt rates in two ways: a thick debris cover (>a few centimeters, or "critical thickness") reduces the ablation rates of the ice underneath due to the low thermal conductivity of debris (Foster et al., 2012; Mihalcea et al., 2008), whereas a thin debris cover (<a few centimeters) accelerates the ice melt rates due to the lower albedo of the supra-glacial debris compared to clean ice (Kayastha et al., 2000; Singh et al., 2000b). The "critical thickness" is the thickness above which ice melt is substantially reduced due to insulation of the supraglacial debris (Brock et al., 2010). Parameterizing melt under the debris cover is therefore difficult due to lack of debris cover thickness measurements, and thus the modeling approach used here does not consider melt under the debris cover. When seasonal snow has melted over debris covered glaciers, melt is generated due to the debris covered glacier albedo, which is generally significantly lower than that of clean glacier ice – which in general would result in larger energy inputs and higher melt rates. Thus, we estimate this approach to work best for glacier ablation areas which are covered by a thin debris cover (less than the critical thickness), where melt is governed by albedo.

For this study, the UEB model was reconfigured to run on a distributed grid to explicitly represent spatial variability in the inputs across a basin, and the enhanced model is referred to in this paper as UEBGrid. The new gridded version of the UEB model facilitates coupling with EPA BASINS and the forcing by inputs from NASA remote sensing and earth science data products such as, satellite

**Table 2**
UEBgrid model inputs, outputs, and state variables. The inputs include static distributed parameters and dynamic meteorological data.

| Dynamic inputs | Static inputs | Output fluxes | State variables |
|---|---|---|---|
| Incoming shortwave radiation | Elevation | Latent heat flux | Snow energy content |
| Incoming longwave radiation | Vegetation cover | Sensible heat flux | Snow water content |
| Air temperature | Vegetation height | Ground heat flux | Snow age |
| Average wind speed | Soil bulk density | Snow temperature | |
| Precipitation | | Melt advected energy | |
| Relative humidity | | Melt outflow flux | |
| Atmospheric pressure | | | |

data (MODIS, ASTER, SRTM), reanalysis data (MERRA) and climate model output (RFE2). UEBGrid was integrated into the HIMALA BASINS software to facilitate the linking to other models, such as GeoSFM, and to take advantage of BASINS' capability to manage input data and visualize results. UEBGrid has adopted a structured file-based input/output format using text and NetCDF files to facilitate its use and incorporation into the HIMALA BASINS software. The UEB model has never before had a graphical user interface and its incorporation into BASINS here has provided graphical user interface capability for UEB thereby making is accessible to a broader group of users.

In UEBGrid, a watershed is divided into a mesh of grid cells and the model runs individually for each grid cell and computes snow or glacier melt. Outflow is then aggregated over sub-basins derived from a Digital Elevation Model (DEM) and used as input into a hydrologic model (in this case, GeoSFM described below, Section 3.3.

### 3.3. GeoSFM streamflow model

The Geospatial Stream Flow Model (GeoSFM), originally developed to work within ESRI's ArcView 3.x software, is a streamflow model developed at the U.S. Geological Survey for the monitoring of hydrologic conditions and the identification of streamflow anomalies (Artan et al., 2007). The monitoring activities include topographic analysis, data assimilation, and time series processing and analysis. In data-sparse regions of the world, GeoSFM is designed to use remotely sensed meteorological data, many of which are in raster format, requiring the adoption of a customizable geographic information system with raster functionality (Artan et al., 2007). Input data consist of elevation, topography, land cover, and soil information to derive and parameterize the sub-basins. Forcing data for the model includes daily estimates of precipitation and potential evapotranspiration to predict daily streamflow at in-situ gauge stations. GeoSFM consists of four modules-preprocessing, hydrologic analysis, parameter calibration, and post-processing. The components of the GeoSFM that are easily accessed through a series of tabs in HIMALA BASINS are: *Terrain Analysis*, *Basin Characteristics*, *Basin Response*, *Rain/Evap Data*, *Compute Soil Water Balance*, *Compute Stream Flow*, *Sensitivity Analysis*, *Model Calibration*, and *Output Results*. HIMALA BASINS allows access to the other hydrological models currently supported by BASINS, along with extending some of the pre-processed datasets to a global extent to enable users outside of the United States to benefit from the modeling framework. To find out more about BASINS, visit http://water.epa.gov.

## 4. Results and discussion: Langtang Khola case study

### 4.1. Model set-up

The integrated HIMALA BASINS model was run for the Langtang Khola watershed in Nepal Himalaya (Fig. 1). Terrain analysis was performed to delineate the sub-basins and flow layers based on the SRTM elevation data using the built-in MapWindow TauDEM tools (Tarboton and Ames, 2001). The Langtang Khola watershed was divided into 24 sub-basins based on hydrologic tools and the SRTM DEM. Fig. 4 indicates the glacier subtype for each sub-basin, with a detailed insets for sub-basins 3, which is an upper glacierized basin containing Langtang glacier. Basin characterization and hydrograph response steps follow to account for the soil and land cover types that fall within each sub-basin and influence the hydrology of that corresponding area. The process continues to the hydrologic analysis stage, including the selection of precipitation/melt and potential evapotranspiration (PET) time series data assigned to the corresponding sub-basin based on sub-basin ID. In this case, the UEBGrid-derived SWIT (total outflow) was selected as the forcing dataset and the PET was automatically estimated using downscaled MERRA air temperature. The soil water balance is then computed using either a linear or a non-linear soil model. For the Langtang case study, the non-linear option was used since it is more suitable for high spatial or temporal resolution analysis and when a model needs to be well calibrated with observed data. Once this is complete, streamflow is computed using one of three routing options (Simple Lag, Diffusion Analog, and Muskingum Cunge). The Muskingum Cunge method was used in this study since it has more parameters and it can diffuse the hydrograph. HIMALA BASINS provides the user not only the option to run both UEBGrid and GeoSFM separately, but to run both models seamlessly in an integrated fashion using the UEBGrid melt output as input for modeling streamflow in GeoSFM.

The GeoSFM-simulated streamflow was estimated using eight years of data, October 1, 2003–September 30, 2010 hydrologic year, and was compared to observed gauge stream flow data from Kyangjing station (3920 m) provided by the Nepal Department of Hydrology and Meteorology (DHM), Nepal. Once the calibrated streamflow run was complete, the post-processing module steps were implemented through the calculation of flow statistics, and the creation of flow maps and hydrographs.

### 4.2. Model results

Modeled results were mapped within HIMALA BASINS depicting status of streamflow and soil water conditions. ASTER-derived substrate type (glacier or ground) and albedo are shown in Fig. 3. The substrate albedo over the clean glacier parts ranged from 0.17 to 0.87 with an average of 0.56, while the substrate albedo over the debris covered glacier parts ranged from 0.15 to 0.71, with an average of 0.26.

In Fig. 5a, we illustrate the UEBGrid derived outflow components: glacier melt, snowmelt and rainfall, as well as GeoSFM simulated streamflow for test sub-basin 3. Fig. 5a illustrates patterns of glacier and snowmelt occurring in sub-basin 3, a highly glacierized upper sub-basin at the headwaters of Langtang glacier. We note that periods of snowmelt occur throughout the year in this region of the Himalaya, whereas glacier melt occurs from May to September, with low flow from October to April. In Fig. 5b, hydrologic components aggregated from all of the sub-basins are shown

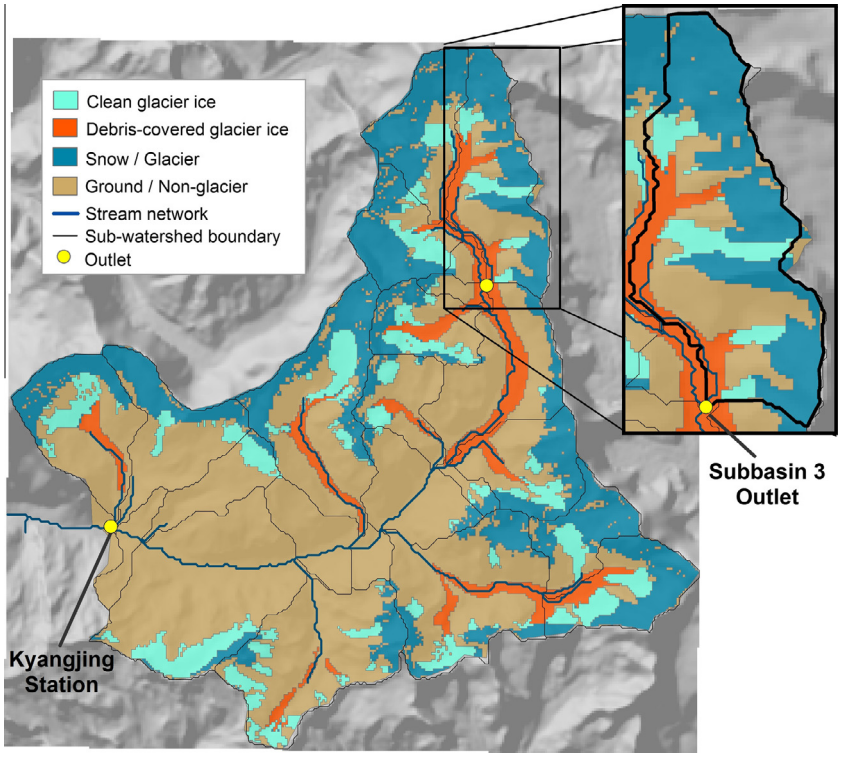


**Fig. 4.** A map of Langtang Khola showing glacier subtype characteristics for each subbasin with an inset for subbasins 3, an upper glacierized basin containing Langtang glacier. The Kyangjing station is labeled as well to indicate the stream flow gauge location used during GeoSFM model calibration.

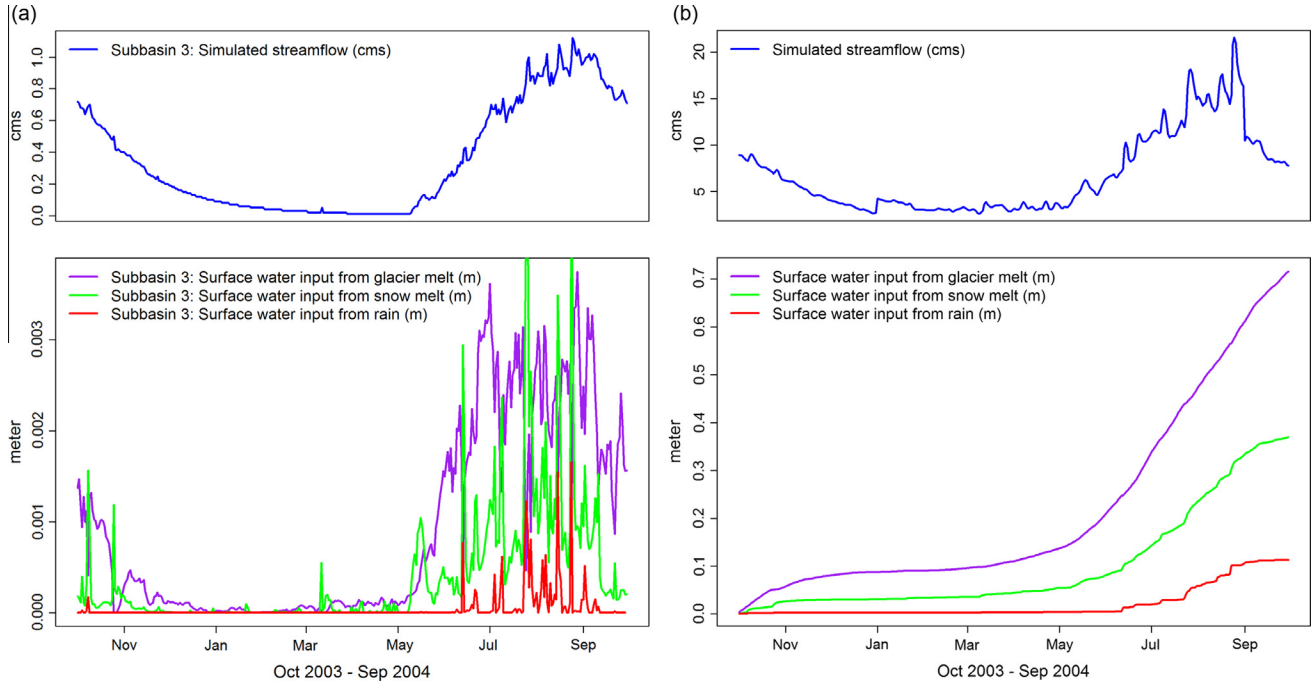


**Fig. 5.** (a) Hydrograph produced in HIMALA BASINS depicting the breakdown of UEBGrid-derived contributions for Langtang Khola glacierized subbasin 3 for 2004 water year. Purple lines depict glacier-melt (SWIGM); green lines depict snowmelt (SWISM), and red lines depict surface water input due to rainfall (SWIR). (b) Hydrographs produced in HIMALA BASINS depicting the cumulative aggregate of UEBGrid-derived surface water contributions for all Langtang Khola subbasins in the form of glacier-melt, snowmelt, and rainfall. Simulated streamflow from GeoSFM is presented on the upper portion of the graph for both figures. (For interpretation of the references to color in this figure legend, the reader is referred to the web version of this article.)

for the 2004 water year. In Table 3, we present hydrologic components aggregated from all of the sub-basins and averaged across the eight years of simulation (2003–2010).

The annual average aggregate surface water input of 1.18 m/year (Table 3) originated 30% from snow melt (SWISM), 62% from glacier melt (SWIGM – both debris covered and clean ice) and 8% from rain

**Table 3**
Langtang Khola watershed hydrologic components estimated by the UEB model averaged for 2003–2010.

| Component | meters/yr |
|---|---|
| Surface water input from rain SWIR | 0.09 |
| Surface water input from snow melt SWISM | 0.35 |
| Surface water input from glacier melt SWIGM | 0.74 |
| Total surface water input SWIT | 1.18 |
| Spatially averaged snow water equivalent SWE accumulation | 0.18 |
| Precipitation | 0.80 |
| Measured streamflow | 0.63 |
| Simulated streamflow | 0.66 |
| Sublimation | 0.20 |

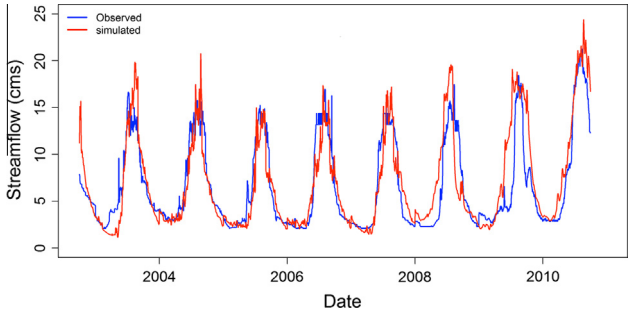


**Fig. 6.** Hydrograph from 2003 to 2010 produced in HIMALA BASINS comparing GeoSFM-derived simulated streamflow with observed (gauge) data collected at the Kyangjing station indicated in Fig. 4.

on bare ground or glacier (SWIR). Under the assumption that the conversion from surface water input to streamflow retains the same proportions, this is in relative agreement with other recent estimates based on a degree-day or ablation model (Racoviteanu et al., 2013; Immerzeel et al., 2012). Racoviteanu et al. (2013) reported 58.3% of streamflow measured at Kyangjing to glacier snow and ice melt, using a simple ablation model. UEB results are also in close agreement with another recent study (Pradhananga et al., 2014), which estimated a contribution of snow and ice melt of 54.3% for the period 1993–2006 in the same basin, using a degree-day model. It is notable that while only 8% of the total watershed is covered by supra-glacial debris,, in our model debris-covered ice contributed about 52% of total surface water, with this 52% originating 47% as glacier melt, 1.4% as rain on the glacier surface and 3.6% from melting of snow on the debris covered surface. This is in contrast with results from Racoviteanu et al. (2013), which obtained a smaller contribution of debris-covered glacier ice (17.7%) compared to clean ice (40.6%) in Langtang Khola. Our study shows a significant excess of meltwater from debris-covered areas, which we speculate it is due to the occurrence of debris covered glacier tongues at low elevations, and particularly due to the low albedo of the debris covered surfaces. This has been recently confirmed in a study by Fujita and Sakai (2014), which also obtained a large amount of meltwater from debris covered areas in Nepal Himalaya (Tso Rolpa glacier). A sensitivity analysis showed that the excess of meltwater in their study was indeed generated at lower elevations over debris covered tongues, and was accelerated due to low albedo. Our results are consistent with Fujita and Sakai (2014). We also note that patterns on glacier melt of debris-covered tongues are highly variable from one area to the other, depending on debris thickness and albedo. As discussed in Section 3.2, in this study we do not take into consideration melt under the debris cover, and the potential insulating effect of the debris cover, which would reduce the ice melt, as noted in other studies (Mihalcea et al., 2008; Brock et al., 2010; Fujita and Sakai, 2014).

In spite of these limitations, we note on Fig. 6 that aggregated simulated discharge from GeoSFM (5.31 m) is in agreement with measured discharge (5.02 m), indicating that the combined models produce a reasonable aggregate water balance. The runoff ratio, based on measured discharge and modeled surface water inputs (5.02/9.43) is 0.53 with the remaining surface water input being the combination of loss to evaporation and change in storage, or due to errors in the surface water input. Furthermore, a comparison between simulated streamflow and observed streamflow for the entire Langtang Khola watershed (Fig. 6) shows that overall, the model captures the hydrologic pattern in this area of the Himalaya, with low flow during the winter months (November to March), and high flow during the monsoon months (June–September). Both the observed and simulated streamflow curves show periods of low and high flows; however, the simulated runs are generally higher than the observed ones, and produce some spikes of high flow during the monsoon, that are not present in the observed data. These overestimates may be due to inaccuracies in the input climate data or problems with the UEB or GeoSFM model, or a combination of these. The largest likely source of error is the climate data, which is entirely derived from satellite and modeled data products.

## 5. Summary and conclusions

In this study, we presented a modeling system (HIMALA BASINS) developed within the framework of HIMALA project to better understand the current contribution of snow and ice melt to streamflow and enable an assessment of the impact of changing climate in the high Himalaya. The UEB snowmelt model was extended to include a capability to simulate glacier melt. It was reconfigured to run on a grid for integration into BASINS. The UEB-Grid model and GeoSFM have been added to the BASINS toolset and coupled to estimate the contributions of glacier, snow melt and rain to streamflow in a seamless fashion.

This integrated modeling system was demonstrated using a case study in the Langtang Khola watershed, where model inputs were taken entirely from downscaled remote sensing products available over a remote south Asian region where meteorological observations are scarce. The results indicate the high fraction of contribution to water input from glacier melt (62%) even though this is a small fraction of the watershed area. The discharge from GeoSFM driven by UEBGrid inputs compares favorably to the total discharge measured. There are discrepancies in the detail of the hydrograph between modeled and measured. However considering the scarcity of data and the modeling system being totally driven by remote sensing and global or regional climate products the comparisons are reasonable.

The augmentation of the GeoSFM model with a capability to capture water melt from snow and glacier ice is important for ICIMOD and its member countries, since water stored during the winter as ice and snow is a significant contributor to rivers during the spring and summer in many basins in South Asia (Immerzeel et al., 2009, 2010). Scarcity of data for meteorological parameters necessary to run hydrological models is a problem in regions at risk of natural hazards such as landslides, floods, droughts and food insecurity (Artan et al., 2007; Brown and Funk, 2008; Sanyal and Lu, 2004). If downstream communities are not aware of excessive temperatures causing snow and ice melt, or of extreme precipitation events, then they will be poorly prepared for changes in river flow after the fact. Using satellite-derived datasets to drive hydrological models in regions without universally available ground observations helps overcome this problem.

## Acknowledgements

This work was supported by a grant from the National Aeronautics and Space Administration's Applied Sciences Program through its 2008 Decision Support through Earth Science Research Results Grant Number NNH08ZDA001N-DECISIONS. A. Racoviteanu's post-doctoral studies were supported by the Centre National d'Etudes Spatiales (CNES), France. This publication was made possible through partial support provided by the Office of U.S. Foreign Disaster Assistance, Bureau for Democracy, Conflict and Humanitarian Assistance, U.S. Agency for International Development, under the terms Award No. AID-OFDA-T-11-00002. The opinions expressed in this publication are those of the authors and do not necessarily reflect views of the U.S. Agency for International Development.

## References

Artan, G. et al., 2007. Adequacy of satellite derived rainfall data for stream flow modeling. Nat. Hazards 43 (2), 167–185.

Asante, K.O., Artan, G.A., Pervez, S., Bandaragoda, C., Verdin, J.P., 2007. Technical manual for the geospatial stream flow model (GeoSFM). In: Sioux Falls, SD, USGS.

Barnett, T.P., Adam, J.C., Lettenmaier, D.P., 2005. Potential impacts of a warming climate on water availability in snow-dominated regions. Nature 438, 303–309.

Bates, D. et al., 2012. R: A Language and Environment for Statistical Computing. The R Project, Auckland, Australia.

Bookhagen, B., Burbank, D.W., 2010. Toward a complete Himalayan hydrological budget: spatiotemporal distribution of snowmelt and rainfall and their impact on river discharge. J. Geophys. Res.: Earth Surf. 115 (F3), F03019.

Brock, B.W. et al., 2010. Meteorology and surface energy fluxes in the 2005–2007 ablation seasons at the Miage debris-covered glacier, Mont Blanc Massif, Italian Alps. J. Geophys. Res. 115 (D9), D09106.

Brown, M.E., Funk, C.C., 2008. Food security under climate change. Science 319 (5863), 580–581.

CGIAR-CSI, 2004. Void-filled Seamless SRTM Data V1. International Centre for Tropical Agriculture (CIAT). Available from the CGIAR-CSI SRTM 90m Database: <http://srtm.csi.cgiar.org> and <http://www.ambiotek.com/topoview>.

Dobhal, D.P., Gergan, J.T., Thayyen, R.J., 2008. Mass balance studies of the Dokriani Glacier from 1992 to 2000, Garhwal Himalaya, India. Bull. Glacier Res. 25, 9–17.

Foster, L.A., Brock, B.W., Cutler, M.E.J., Diotri, F., 2012. A physically based method for estimating supraglacial debris thickness from thermal band remote-sensing data. J. Glaciol. 58 (210), 677–690.

Friedl, M.A., Sulla-Menashe, D., Tan, B.S.A., Ramankutty, N., Sibley, A.H.X., 2010. Collection 5 global land cover: algorithm refinements and characterization of new datasets. Remote Sens. Environ. 114, 168–182.

Fujita, K., Sakai, A., 2014. Modelling runoff from a Himalayan debris-covered glacier. Hydrol. Earth Syst. Sci. 11, 2441–2482.

Greuell, W., Oerlemans, J., 2004. Narrowband-to-broadband albedo conversion for glacier ice and snow: equations based on modeling and ranges of validity of the equations. Remote Sens. Environ. 89 (1), 95–105.

Greuell, W., Reijmer, C.H., Oerlemans, J., 2002. Narrowband-to-broadband albedo conversion for glacier ice and snow based on aircraft and near-surface measurements. Remote Sens. Environ. 82 (1), 48–63.

Hijmans, Robert J. et al., 2013. Raster: Geographic data analysis and modeling, 2.1–66.

Hock, R., 2003. Temperature index melt modelling in mountain areas. J. Hydrol. 282 (1–4), 104–115.

Hock, R., 2005. Glacier melt: a review of processes and their modelling. Prog. Phys. Geogr. 29 (3), 362–391.

Immerzeel, W., Droogers, P., de Jong, S.M., Bierkens, M.F.P., 2009. Large-scale monitoring of snow cover and runoff simulation in Himalayan river basins using remote sensing. Remote Sens. Environ. 113 (1), 40–49.

Immerzeel, W., van Beek, L.P.H., Bierkens, M.F.P., 2010. Climate change will affect the Asian water towers. Science 328 (5984), 1382–1385.

Immerzeel, W.W., van Beek, L.P.H., Konz, M., Shrestha, A.B., Bierkens, M.F.P., 2012. Hydrological response to climate change in a glacierized catchment in the Himalayas. Clim. Change 110 (3–4), 721–736.

Jeuland, M., Harshadeep, N., Escurra, J., Blackmore, D, Sadoff, C., 2013. Implications of climate change for water resources development in the Ganges basin. Water Policy 15 (1), 26–50.

Kaser, G., Grosshauser, M., Marzeion, B., 2010. Contribution potential of glaciers to water availability in different climate regimes. Proc. Natl. Acad. Sci. USA 107 (47), 20223–20227.

Kayastha, R.B., Ohata, T., Ageta, Y., 1999. Application of mass balance model to a Himalayan Glacier. J. Glaciol. 45 (151), 559–567.

Kayastha, R.B., Takeuchi, Y., Nakawo, M., Ageta, Y., 2000. Practical prediction of ice melting beneath various thickness of debris cover on Khumbu Glacier, Nepal, using a positive degree-day factor. In: Raymond, C.F., Nakawo, M., Fountain, A. (Eds.), Debris-Covered Glaciers. Proceedings from a Workshop held at Seattle, WA, USA, September 2000. IAHS, Wallingford, UK, pp. 71–81.

Knowles, N., Cayan, D.R., 2002. Potential effects of global warming on the Sacramento/San Joaquin watershed and the San Francisco estuary. Geophys. Res. Lett. 29 (18), 38-1–38-4.

Liston, G.E., Elder, K., 2006. A meteorological distribution system for high-resolution terrestrial modeling (MicroMet). J. Hydrometeorol. 7 (2), 217–234.

Lo, Y.-H., Blanco, J.A., Seely, B., Welham, C., Kimmins, J.P., 2011. Generating reliable meteorological data in mountainous areas with scarce presence of weather records: the performance of MTCLIM in interior British Columbia, Canada. Environ. Model. Softw. 26 (5), 644–657.

Lucchesi, R., 2012. File Specification for MERRA Products. GMAO Office Note No. 1 (Version 2.3). 82 pp.

Luce, C.H., 2000. Scale Influences on the Representation of Snowpack Processes. PhD Thesis, Utah State University, Logan, 188 pp.

Luce, C.H., Tarboton, D.G., 2004. The application of depletion curves for parameterization of subgrid variability of snow. Hydrol. Process. 18, 1409–1422.

Luce, C.H., Tarboton, D.G., 2010. Evaluation of alternative formulae for calculation of surface temperature in snowmelt models using frequency analysis of temperature observations. Hydrol. Earth Syst. Sci. 14 (3), 535–543.

Luce, C.H., Tarboton, D.G., Cooley, K.R., 1998. The influence of the spatial distribution of snow on basin-averaged snowmelt. Hydrol. Process. 12 (10–11), 1671–1683.

Mahat, V., Tarboton, D.G., 2012. Canopy radiation transmission for an energy balance snowmelt model. Water Resour. Res. 48, W01534.

Mahat, V., Tarboton, D.G., 2013. Representation of canopy snow interception, unloading and melt in a parsimonious snowmelt model. Hydrol. Process. http://dx.doi.org/10.1002/hyp.10116.

Mahat, V., Tarboton, D.G., Molotch, N.P., 2013. Testing above and below canopy representations of turbulent fluxes in an energy balance snowmelt model. Water Resour. Res. 49 (2), 1107–1122.

Mihalcea, C. et al., 2008. Spatial distribution of debris thickness and melting from remote-sensing and meteorological data, at debris-covered Baltoro glacier, Karakoram, Pakistan. Ann. Glaciol. 48 (1), 49–57.

National Research Council, 2012. Himalayan Glaciers: Climate Change, Water Resources, and Water Security, Washington, DC., doi: 10.3189/2014AoG66A123.

Pradhananga, N.S., Kayastha, R.B., Bhattarai, B.C., Adhikari, T.R.C, Pradhan, S., Devkota, L.P., Shrestha, A.B., Mool, P.K., 2014. Estimation of discharge from Langtang River basin, Rasuwa, Nepal, using a glacio-hydrological model. Ann. Glaciol. 55 (66), 223–230. http://dx.doi.org/10.3189/2014AoG66A123.

Racoviteanu, A., Williams, M.W., Barry, R., 2008. Optical remote sensing of glacier mass balance: a review with focus on the Himalaya. Sensors, Spec. Issue: Remote Sens. Environ. (8), 3355–3383.

Racoviteanu, A., Paul, F., Raup, B., Khalsa, S.J.S., Armstrong, R., 2009. Challenges and recommendations in mapping of glacier parameters from space: results of the 2008 Global Land Ice Measurements from Space (GLIMS) workshop, Boulder, Colorado, USA. Ann. Glaciol. 50 (53), 53–69.

Racoviteanu, A., Armstrong, R., Williams, M., 2013. Evaluation of an ice ablation model to estimate the contribution of melting glacier ice to annual discharge in the Nepal Himalaya. Water Resour. Res. 49 (9), 5117–5133.

Raleigh, M., Lott, F., Lundquist, J., 2008. Most Critical Surface Meteorological Measurements for Modeling Distributed Snowmelt in the Sierra Nevada, California, AGU Fall Meeting Abstracts, pp. 0971.

Rienecker, M.M. et al., 2011. MERRA: NASA's modern-era retrospective analysis for research and applications. J. Clim. 24 (14), 3624–3648.

Sanyal, J., Lu, X.X., 2004. Application of remote sensing in flood management with special reference to monsoon in Asia: a review. Nat. Hazards 33 (2), 283–301.

Savoskul, O.S., Smakhtin, V., 2013. Glacier Systems and Seasonal Snow Cover in Six Major Asian River Basins: Hydrological Role under Changing Climate. International Water Management Institute (IWMI) Research Report 150, Colombo, Sri Lanka.

Schulz, O., De Jong, C., 2004. Snowmelt and sublimation: field experiments and modelling in the High Atlas Mountains of Morocco. Hydrol. Earth Syst. Sci. Discuss. 8 (6), 1076–1089.

Sen Gupta, A., 2014. Improving the physical processes and model integration functionality of an energy balance model for snow and glacier melt. In: Civil and Environmental Engineering. Utah State University, Logan, p. 195.

Shrestha, M.S., 2010. Bias-Adjustment of Satellite-Based Rainfall Estimates over the Central Himalayas of Nepal for Flood Prediction. Kyoto University, Kyoto, Japan.

Singh, P., Kumar, A., 1997a. Effect of orography on precipitation in the Western Himalayan region. J. Hydrol. 199, 183–206.

Singh, P., Kumar, N., 1997b. Impact assessment of climate change on the hydrological response of a snow and glacier melt runoff dominated Himalayan river. J. Hydrol. 193 (1–4), 316–350.

Singh, P., Kumar, N., Arora, M., 2000a. Degree-day factors for snow and ice for Dokriani Glacier, Garhwal Himalayas. J. Hydrol. 235 (1–2), 1–11.

Singh, P., Kumar, N.S.R., Singh, Y., 2000b. Influence of a fine debris layer on the melting of snow and ice on a Himalayan glacier. In: Nakawo, M., Raymond, C.F., Fountain, A. (Eds.), Debris-covered Glaciers. IAHS, Wallingford, pp. 63–69.

Suarez, M.J. et al., 2008. The GEOS-5 Data Assimilation System-Documentation of Versions 5.0.1, 5.1.0, and 5.2.0.

Takeuchi, Y., Kayastha, R.B., Nakawo, M., 2000. Characteristics of ablation and heat balance in debris-free and debris-covered areas on Khumbu Glacier, Nepal Himalayas, in the pre-monsoon season. In: Nakawo, M., Raymond, C.F., Fountain, A. (Eds.), Debris-covered Glaciers. IAHS, Wallingford, pp. 53–61.

Tarboton, D.G., 1994. The source hydrology of severe sustained drought in the Southwestern United States. J. Hydrol. 161, 31–69.
Tarboton, D.G., Ames, D.P., 2001. Advances in the Mapping of Flow Networks from Digital Elevation Data. World Water and Environmental Resources Congress, Orlando, Florida.
Tarboton, D.G., Luce, C.H., 1996. Utah Energy Balance Snow Accumulation and Melt Model (UEB). US Forest Service, Price, Utah.
Tarboton, D., Chowdhury, T., Jackson, T., 1995. A spatially distributed energy balance snowmelt model. In: Tonnessen, K., Williams, M., Tranter, M. (Eds.), Biogeochemistry of Seasonally Snow-Covered Catchments: Proceedings of a Boulder Symposium. IAHS, Boulder, CO, pp. 141–155.
Tarboton, D.G., Blöschl, G., Cooley, K., Kirnbauer, R., Luce, C., 2000. Spatial snow cover processes at Kühtai and Reynolds Creek. In: Grayson, R., Blöschl, G. (Eds.), Spatial Patterns in Catchment Hydrology: Observations and Modelling. Cambridge University Press, Cambridge, pp. 158–186.
Thayyen, R.J., Gergan, J.T., 2010. Role of glaciers in watershed hydrology: a preliminary study of a Himalayan catchment. Cryosphere 4 (1), 115–128.
Wagnon, P., Kumar, Rajesh, Arnaud, Yves, Linda, Anurag, Sharma, Parmanand, Vincent, Christian, Pottackal, Jose, Berthier, Etienne, Ramanathan, Alagappan, Hassnain, Chevalier, Pierre, 2007. Four years of mass balance on Chhota Shigri Glacier, Himachal Pradesh, India, a new benchmark glacier in the western Himalaya. J. Glaciol. 53 (183), 603–611.
Wagnon, P. et al., 2013. Seasonal and annual mass balances of Mera and Pokalde glaciers (Nepal Himalaya) since 2007. Cryosphere.
Wisner, B., Blaikie, P., Cannon, T., Davis, I., 2004. At Risk, second ed. Taylor and Francis Books Ltd, Wiltshire.
Wu, W.-S., Purser, R.J., Parrish, D.F., 2002. Three-dimensional variational analysis with spatially inhomogeneous covariances. Mon. Weather Rev. 130 (12), 2905–2916.
Xie, P., Yarosh, Y., Love, T., Janowiak, J., Arkin, P.A., 2002. A real-time daily precipitation analysis over South Asia. In: 16th Conference on Hydrology. American Meteorological Society, Orlando, FL.
You, J., 2004. Snow Hydrology: The Parameterization of Subgrid Processes within a Physically Based Snow Energy and Mass Balance Model. PhD Thesis, Utah State University, Logan.